



# Somatostatin-immunoreactive neurons of the rat gut during the development

Andrey I. Emanuilov<sup>1</sup> · Antonina F. Budnik<sup>2</sup> · Petr M. Masliukov<sup>1,3</sup>

Accepted: 11 August 2024 / Published online: 17 August 2024

© The Author(s), under exclusive licence to Springer-Verlag GmbH Germany, part of Springer Nature 2024

## Abstract

Somatostatin (SST) is a peptide expressed in the peripheral and central nervous systems, as well as in endocrine and immune cells. The aim of the current study is to determine the percentage of SST immunoreactive (IR) neurons and their colocalization with choline acetyltransferase (ChAT), neuronal nitric oxide synthase (nNOS), neuropeptide Y (NPY), and glial fibrillary acidic protein (GFAP) in the myenteric plexus (MP) and submucous plexus (SP) of the small intestine (SI) and large intestine (LI) of rats across different age groups from newborn to senescence using immunohistochemistry. In the MP of the SI and LI, the percentage of SST-IR neurons significantly increased during early postnatal development from  $12 \pm 2.4$  (SI) and  $13 \pm 3.0$  (LI) in newborn rats to  $23 \pm 1.5$  (SI) and  $18 \pm 1.6$  (LI) in 20-day-old animals, remaining stable until 60 days of age. The proportion of SST-IR cells then decreased in aged 2-year-old animals to  $14 \pm 2.0$  (SI) and  $10 \pm 2.6$  (LI). In the SP, the percentage of SST-IR neurons significantly rose from  $22 \pm 3.2$  (SI) and  $23 \pm 1.7$  (LI) in newborn rats to  $42 \pm 4.0$  in 20-day-old animals (SI) and  $32 \pm 4.9$  in 30-day-old animals (LI), before declining in aged 2-year-old animals to  $21 \pm 2.6$  (SI) and  $28 \pm 7.4$  (LI). Between birth and 60 days of age, 97–98% of SST-IR neurons in the MP and SP colocalized with ChAT in both plexuses of the SI and LI. The percentage of SST/ChAT neurons decreased in old rats to  $85 \pm 5.0$  (SI) and  $90 \pm 3.8$  (LI) in the MP and  $89 \pm 3.2$  (SI) and  $89 \pm 1.6$  (LI) in the SP. Conversely, in young rats, only a few SST-IR neurons colocalized with nNOS, but this percentage significantly increased in 2-year-old rats. The percentage of SST/NPY-IR neurons exhibited considerable variation throughout postnatal development, with no significant differences across different age groups in both the MP and SP of both intestines. No colocalization of SST with GFAP was observed in any of the studied animals. In conclusion, the expression of SST in enteric neurons increases in young rats and decreases in senescence, accompanied by changes in SST colocalization with ChAT and nNOS.

**Keywords** Somatostatin · Enteric nervous system · Immunohistochemistry · Development

## Introduction

Somatostatin (SST) is a peptide expressed in the peripheral and central nervous system, endocrine, and immune cells (Brazeau et al. 1973; Kumar 2023). SST exists in two

functionally active isoforms, namely SST14 and SST28, which are derived from a common precursor, preprosomatostatin (Warren and Shields 1984; Ampofo et al. 2020). SST also serves as a neurotransmitter and neuromodulator in the CNS. It inhibits the release of hormones, cytokine, growth factor, and cell proliferation. SST has also been identified in the enteric nervous system of mammals (Furness 2006; Gonkowski and Rytel 2019).

Approximately 90% of SST in the gut is located in the enteroendocrine cells, with only 10% found in the enteric nervous system. Despite the majority being located in endocrine cells, SST still serves crucial functions within the enteric nervous system, both under normal circumstances and in disease states (Penman et al. 1983; Gonkowski and Rytel 2019). SST immunoreactive (IR) neurons in the enteric nervous system of the gut inhibit intestinal motility,

✉ Petr M. Masliukov  
mpm@ysmu.ru

<sup>1</sup> Department of Human Anatomy, Yaroslavl State Medical University, Yaroslavl, Russia

<sup>2</sup> Department of Normal and Pathological Anatomy, Kabardino-Balkarian State University Named After H.M. Berbekov, Nalchik, Russia

<sup>3</sup> Department of Normal Physiology and Biophysics, Yaroslavl State Medical University, Revolucionnaya 5, Yaroslavl, Russia 150000

secretion, and inflammation (Van Op den Bosch et al. 2009; Gonkowski and Rytel 2019).

Distinctions are observed in the number of SST-IR neurons in the enteric ganglia of different species. In the small intestine (SI) of the guinea pig, 5% of neurons in the myenteric plexus (MP) and 17% in the submucous plexus (SP) are SST-IR. Similar results were shown for the large intestine (LI) (Costa et al. 1980). In the colon of the domestic pig, only a small percentage of neurons in the MP and SP are SST-IR (Gonkowski and Calka 2010). In the rat ileum and jejunum, 18% of neurons in the SP are SST-IR (Pataky et al. 1990), and 1–6 neurons per ganglion in the colon myenteric plexus of rats and mice contain SST (Heinicke and Kiernan 1990).

The majority of enteric neurons utilize acetylcholine as the main neurotransmitter, which is synthesized by the enzyme choline acetyltransferase (ChAT). Another population of neurons contains the enzyme neuronal nitric oxide synthase (nNOS) for nitric oxide (NO) synthesis. ChAT-containing neurons are excitatory cells, while nNOS neurons are part of inhibitory motor neurons or interneurons (Furness 2006; Furness and Stebbing 2018). In adult rats, nNOS-IR neurons have been identified in the myenteric plexus (MP) (Budnik and Masliukov 2023). However, in the submucous plexus (SP), many neurons colocalize ChAT with neuropeptide Y (NPY) (Furness 2006).

It has been established that the neurochemistry of enteric neurons changes during postnatal development (Hao and Young 2009; Foong 2016; Masliukov et al. 2017a, b, 2023; Scott-Solomon et al. 2021). SST is transiently expressed in embryonic sympathetic neurons (Masliukov et al. 2023). However, there are limited data available regarding the developmental changes of SST-IR enteric neurons in the postnatal period. The aim of the current study is to investigate changes in the location and percentage of SST-IR neurons, as well as the colocalization of SST with other neurotransmitters and the glial marker glial fibrillary acidic protein (GFAP) in rats of different ages using immunohistochemistry.

## Experimental procedures

### Animals

Experiments were performed on male Wistar rats at various ages: 1 day, 10 days, 20 days, 30 days, 60 days, and 2 years old, with each age group consisting of five animals. The young rats were kept with their mothers and siblings until weaning at day 30. The rats were given unlimited access to food and were housed in a controlled environment at 20–22 °C with 40–70% humidity on a 12:12 h light–dark cycle. All animal procedures were carried out in compliance

with the regulations of the Local Ethics Committee of Yaroslavl State Medical University, as detailed in protocol no. 60, dated 16 February 2023.

### Tissue preparation

Rats were euthanized with an overdose of urethane (3 g/kg, i.p.) before being perfused through the heart with 500 ml of saline solution containing 1 ml of heparin and a fixative solution consisting of 4% paraformaldehyde in 0.1 M phosphate buffer. Pieces of the small intestine (proximal duodenum) and large intestine (mid colon) were then carefully isolated after perfusion and treated with the same fixative for 1–2 h at room temperature. In one type of experiment, the mucosa and submucosa were removed to expose the MP, while in the other, the muscularis externa and serosa were excised to visualize the intact SP.

After the fixation process, tissue samples underwent three 30-min washes in 0.01 M phosphate-buffered saline (PBS) (pH 7.4), followed by cryoprotection through overnight immersion in a 20% sucrose solution (pH 7.4) at 4 °C. The samples were then embedded in Tissue-Tek® O.C.T. Compound (Sakura Finetek Europe, the Netherlands), placed on a cryostat chuck, and frozen. Subsequently, 14- $\mu$ m-thick sections were sliced using a cryotome (Shandon E, Thermo Fisher Scientific, UK) and mounted on glass SuperFrost™ Plus slides (Thermo Fisher Scientific, UK).

### Immunohistochemistry

The tissue slices were blocked with a buffer comprising 5% normal donkey serum (Jackson ImmunoResearch Laboratories, USA) and 0.3% Triton X-100 (Sigma, USA) in PBS at room temperature for a half an hour. Double immunostaining with antibodies from different host species (Table 1) was used to identify SST, nNOS, ChAT, NPY, and GFAP. An antibody targeting PGP9.5 was applied to label the entire population of enteric ganglionic neurons.

Subsequently, the sections were treated with the primary antisera overnight at room temperature, followed by rinsing in PBS and additional incubation with the appropriate secondary antisera (Table 1) for 2 h at room temperature. After three additional PBS rinses, the sections were coverslipped with VECTASHIELD® Antifade Mounting Medium (Vector Bioproducts, USA).

Two distinct steps were undertaken to assess the specificity of the antibodies. In the first step, which served as a negative control, sections that were not exposed to primary antibodies were stained. The second step involved preabsorption of the primary antibodies with an excess amount of the specific immunogen peptide (Table 2) at a concentration of 0.25 mg/ml for 2 h prior to the incubation process at room

**Table 1** Primary and secondary antisera used for immunohistochemistry

Antisera	Host species	Dilution	Source
Primary			
SST	Goat	1:300	Santa Cruz, sc-7819, lot F1609
SST	Rabbit	1:300	Abclonal, A9274, lot 5500009967
nNOS	Rabbit	1:300	Abcam, ab15203, lot GR90846-1
PGP9.5	Guinea pig	1:200	Abcam, ab10410, lot GR3209499-22
NPY	Rabbit	1:500	Abcam, ab30914, lot GR3213170-1
ChAT	Goat	1:100	Millipore, AB144p, lot 3067431
GFAP	Goat	1:300	Abcam, ab53554, lot GR3307240-1
Secondary			
Anti-goat IgG FITC	Donkey	1:200	Jackson Immunoresearch, code 705–095-147
Anti-goat IgG CY3	Donkey	1:200	Jackson Immunoresearch, code 705–165-147
Anti-rabbit IgG FITC	Donkey	1:200	Jackson Immunoresearch, code 711–095-152
Anti-rabbit IgG CY3	Donkey	1:200	Jackson Immunoresearch, code 711–165-152
Anti-guinea pig IgG FITC	Donkey	1:200	Jackson Immunoresearch, code 706–095-148

**Table 2** Immunogen peptides used for reabsorption with primary antibodies

Primary antisera	Immunogen peptide
SST	Abcam, ab141206
nNOS	Abcam, ab22863
PGP9.5	Abcam, ab198431
NPY	Abcam, ab112330
ChAT	Millipore, AG220MI
GFAP	Abcam, ab114149

temperature. No positive immunoreactivity was observed in any of the control sections.

### Characteristics of antibodies

The polyclonal antibody to SST (Santa Cruz, sc-7819) has been used in numerous works, including studies of the central nervous system and endocrine glands (34 articles on PubMed). The immunogen for this antibody was a synthetic peptide LELQRSANSNPAMAPRERK, mapping amino acids 84–102 of human SST. Western blot analysis of mouse brain lysates immunostained with this antibody revealed a molecular weight of 17 kDa (Real et al. 2009), which aligned with the manufacturer's reported value. In our previous work (Vishnyakova et al. 2021), the staining pattern obtained with this antibody in rat hypothalamus was identical to the study with the same antibody (Kiss et al. 2006) and another rabbit SST antiserum (Foo et al. 2014). Additionally, SST immunoreactivity was completely absent in brain sections from SST knockout mice processed with this antibody (Lepousez et al. 2010).

Another SST antibody (Abclonal, A9274) has been employed in multiple studies. According to the datasheet,

the immunogen for this antibody is a recombinant fusion protein encompassing a sequence from amino acids 23–116 of human SST. Immunoblots using this antibody on the rat brain (Yu et al. 2020) showed a distinct band corresponding to the expected size of 17 kDa, consistent with the product datasheet. In our study, the immunohistochemical staining with this antibody was similar to that obtained with the Santa Cruz sc-7819 antibody, as mentioned above. In other works, such as those on the spinal cord, the staining pattern achieved with this antibody (Zhang et al. 2024) resembled experiments where SST neurons were genetically targeted (Fatima et al. 2019).

The nNOS antibody (Abcam, ab15203) has been described in various studies. According to the datasheet, the immunogene for this antibody is a synthetic peptide within mouse nNOS (C terminal). The specificity of the nNOS antibody was tested by western blotting of mouse brain homogenates (Fazi et al. 2010). Previously, we used this type of antibody to label sensory nNOS neurons in the rat dorsal root ganglia using immunohistochemistry (Masliukov et al. 2014). The results obtained were similar to those achieved using other nNOS antibodies in that study, as well as in other works (Islam et al. 2020).

The results obtained using the guinea-pig PGP9.5 antibody (Abcam, ab10410) have been described in multiple studies. The immunogen for this antibody was a synthetic peptide GASSEDLLKDKAAKVCL, corresponding to amino acids 175–191 of the soluble human cytoplasmic protein PGP9.5. We previously used this antibody to label the whole population of neurons in the enteric ganglia using immunohistochemistry (Budnik and Masliukov 2023). The results were comparable with the studies where another rabbit PGP 9.5 antibody was employed (Barrenschee et al. 2015).

Rabbit polyclonal NPY antibody (Abcam, ab30914) has been employed in multiple studies (61 on PubMed). The specificity of this antibody was tested in NPY knockout and control mice using immunohistochemistry (Peng et al. 2023; Cao et al. 2022) and western blotting (Cao et al. 2022).

The goat polyclonal antibody to ChAT of a peripheral type (AB144p, Millipore) is commonly used to label enteric cholinergic neurons using immunohistochemistry and western blotting (Mongardi Fantaguzzi et al. 2009; Hao et al. 2013; Machado et al. 2023). This antibody was raised against the human placental enzyme and recognizes a protein of 70–74 kDa in mouse brain lysates on western blotting, according to the manufacturer's information.

The goat polyclonal GFAP antibody (Abcam, ab53554) has been employed in numerous studies (217 on PubMed). The immunogen for this antibody was a synthetic peptide corresponding to human GFAP amino acids 417–430 (C-terminal). This antibody has been validated in various immunohistochemical and western blotting studies (Rosas-Arellano et al. 2016; Xu et al. 2016). Ab53554 has also been used to identify enteric glial cells through immunohistochemistry (Guyer et al. 2023). In this study, GFAP expression was further confirmed using *in situ* hybridization.

## Image processing and statistics

The samples were analyzed under Olympus upright fluorescence microscope model BX43 (Olympus, Japan), which was equipped with U-FBWA (blue excitation) and U-FGWA (green excitation) filter cubes. Olympus UPLFLN 20X Objective was normally used (Olympus UPLFLN U Plan Fluorite 20X/0.50  $\infty$ /0.17/FN 26.5). A color-cooled CMOS Camera (FL 20) and Mosaic V2.1 imaging software (Tucsen, China) were used to obtain images.

To estimate the percentage of SST-IR neurons, the total number of PGP-IR cells in the measured area was determined and considered as 100%. IR profiles were analyzed distinctly in the MP and SP of the SI and LI. The cross-section area, the number of neurons, and the intensity of the immunofluorescence were assessed in arbitrarily selected measured zones where microscopic field area was 0.12 mm<sup>2</sup> at 200 $\times$  magnification by ImageJ (NIH image program, version 1.53 k). Pearson's correlation and Manders' overlap coefficient (MC) were utilized for colocalization analysis using the JACoP plugin for ImageJ software, following the methods outlined in Bolte and Cordelières (2006) and Dunn et al. (2011). Records from ten examined areas per plexus per age category per animal were collected, and the results from animals in each age group were combined, resulting in group sizes of  $n = 5$ . The immunofluorescence intensity

was assessed by calculating the mean gray value within a range of 0–255.

Statistical analysis was carried out with Sigma Plot 12 software (Systat Software, USA). The data were expressed as the mean  $\pm$  standard deviation (SD). The normality of the distribution was assessed using the Shapiro–Wilk test. To compare the means, a one-way analysis of variance (ANOVA) was conducted, and post hoc Tukey's test for multiple comparisons was applied. Statistical significance was determined at  $p < 0.05$ .

## Results

The results have shown that SST-IR neurons were present in the MP and SP of SI and LI in rats from birth through senescence (Fig. 1). The SST-positive granular elements were observed surrounding the non-immunoreactive nucleus in the cytoplasm, with SST-IR fibers forming a network around other enteric neuronal cells in the ganglia of both the SI and LI.

### SST/PGP9.5 colocalization

Regarding the colocalization of SST with PGP9.5, which is a pan-neuronal marker, it was found that all SST-IR cells also expressed PGP9.5. In the MP of both the SI and LI, the percentage of SST-IR neurons significantly increased during early postnatal development, rising from  $12 \pm 2.4$  (SI) and  $13 \pm 3.0$  (LI) in newborn rats to  $23 \pm 1.5$  (SI) and  $18 \pm 1.6$  (LI) in 20-day-old animals ( $p < 0.001$ , SI;  $p = 0.039$ , LI). These levels remained relatively stable until 60 days of age (Figs. 1 and 2). However, the proportion of SST-IR cells significantly decreased in 2-year-old rats, dropping to  $14 \pm 2.0$  (SI) and  $10 \pm 2.6$  (LI) compared with 20-day-old ( $p < 0.001$ ), 30-day-old ( $p < 0.001$ ), and 60-day-old rats ( $p = 0.001$ ) in the SI, and compared with 60-day-old rats ( $p = 0.012$ ) in the LI.

In the SP, the percentage of SST-IR neurons also significantly increased during early postnatal development, starting from  $22 \pm 3.2$  (SI) and  $23 \pm 1.7$  (LI) in newborn rats and reaching  $42 \pm 4.0$  in 20-day-old animals (SI) and  $32 \pm 4.9$  in 30-day-old animals (LI) ( $p < 0.001$ , SI;  $p = 0.039$ , LI). Similar to the MP, these levels remained steady until 60 days of age. Yet, the proportion of SST-IR cells decreased significantly in 2-year-old rats, declining to  $21 \pm 2.6$  (SI) and  $28 \pm 7.4$  (LI) compared with 20-day-old ( $p < 0.001$ ), 30-day-old ( $p = 0.029$ ), and 60-day-old rats ( $p = 0.025$ ) in the SI and compared with 30-day-old ( $p = 0.005$ ) and 60-day-old rats ( $p = 0.015$ ) in the LI.

The number of PGP-IR neurons per ganglion remained constant during development in the MP, with values varied

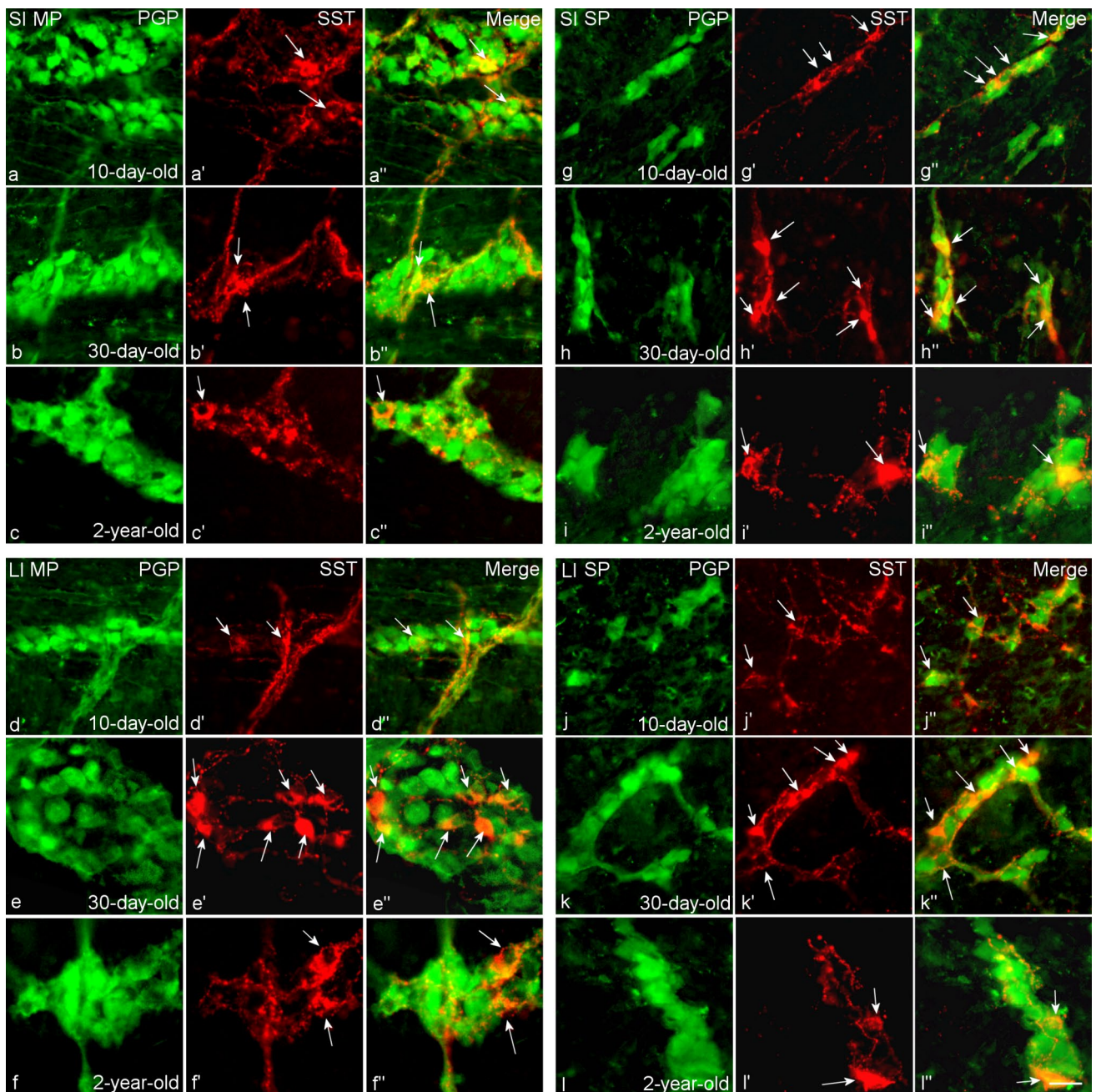


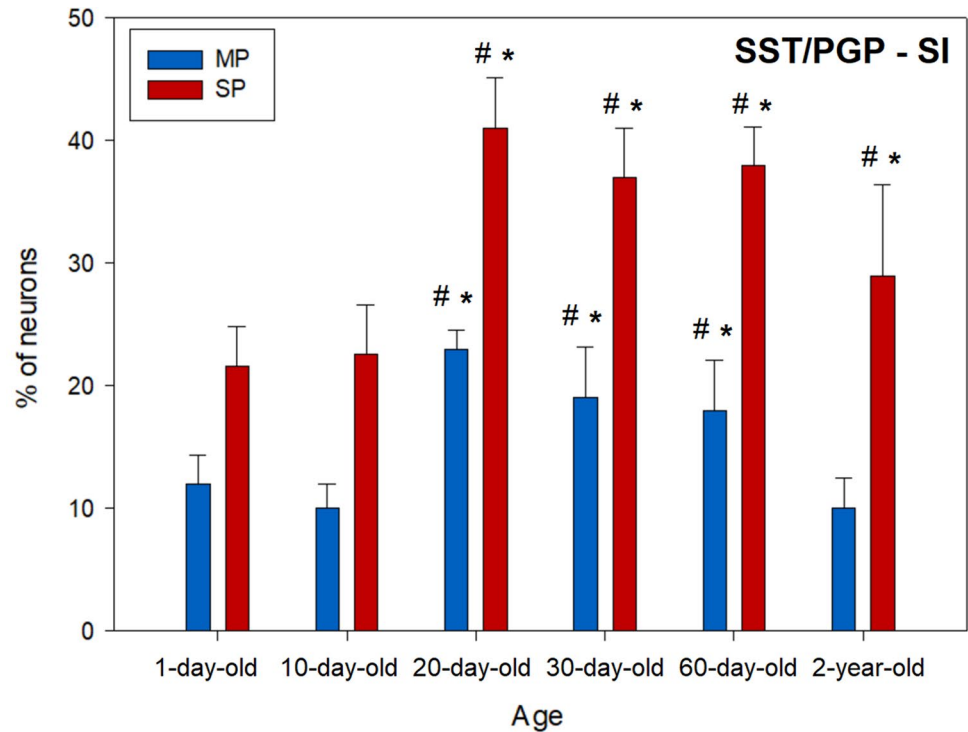
**Fig. 1** Fluorescence micrographs of SST (red) and PGP9.5 (green) immunoreactivity in the MP (a–f) and SP (g–l) of SI (a–c, g–i) and LI (d–f, j–l) of 10-day-old (a, g, d, j), 30-day-old (b, h, e, k), and 2-year-old (c, f, i, l) rats. A letter without an apostrophe represents the

green channel, a letter with one apostrophe (') indicates the red channel, and a letter with two apostrophes (") denotes the merged image. SST-IR neurons are marked with arrows. Scale bar, 30 μm

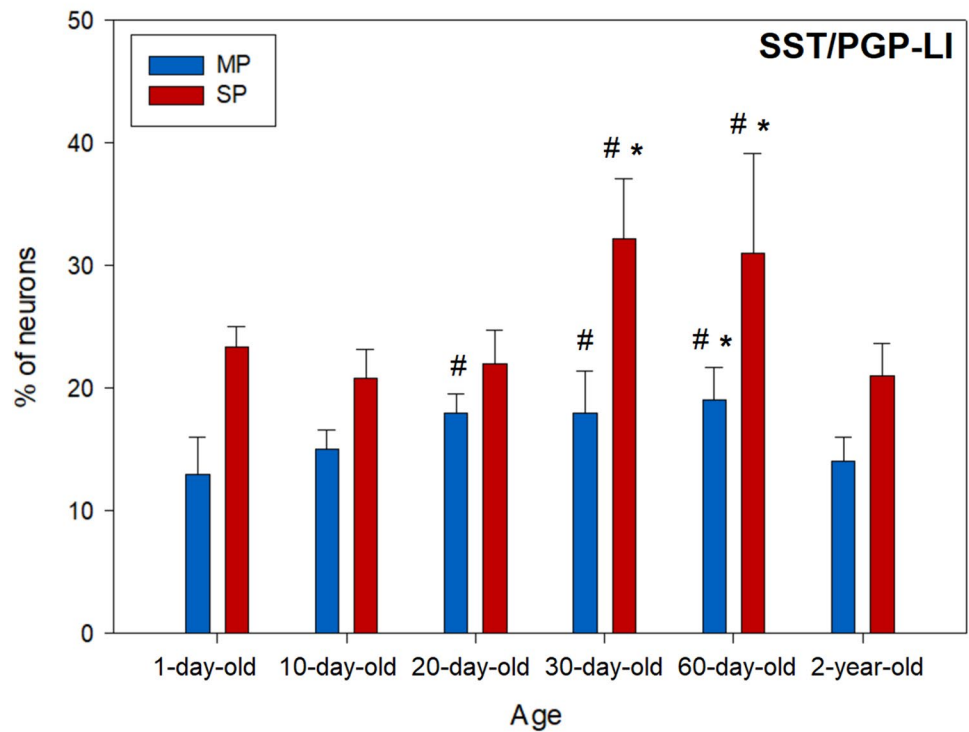
between  $20.5 \pm 3.0$  and  $21.5 \pm 3.3$  in both SI and LI. However, in the SP of newborn rats, we found fewer PGP-IR neurons ( $6.2 \pm 0.6$  SI and  $6.8 \pm 0.5$  LI) compared with 10-day-old rats ( $10.4 \pm 1.2$  SI and  $11.3 \pm 1.4$  LI) ( $p < 0.05$ ).

We did not detect statistically significant differences in the number of PGP9.5-IR neurons in the SP between 10-day-old rats and older rats in either the SI or LI.

**Fig. 2** The percentage of SST-IR neurons in the SI (a) and LI (b) of rats at various ages.  $N=5$  in each age group (6 groups: 1-, 10-, 20-, 30-, 60-day-old and 2-year-old rats). One-way ANOVA, # $p < 0.05$  compared with newborn rats, \* $p < 0.05$  compared with 2-year-old rats



a



b

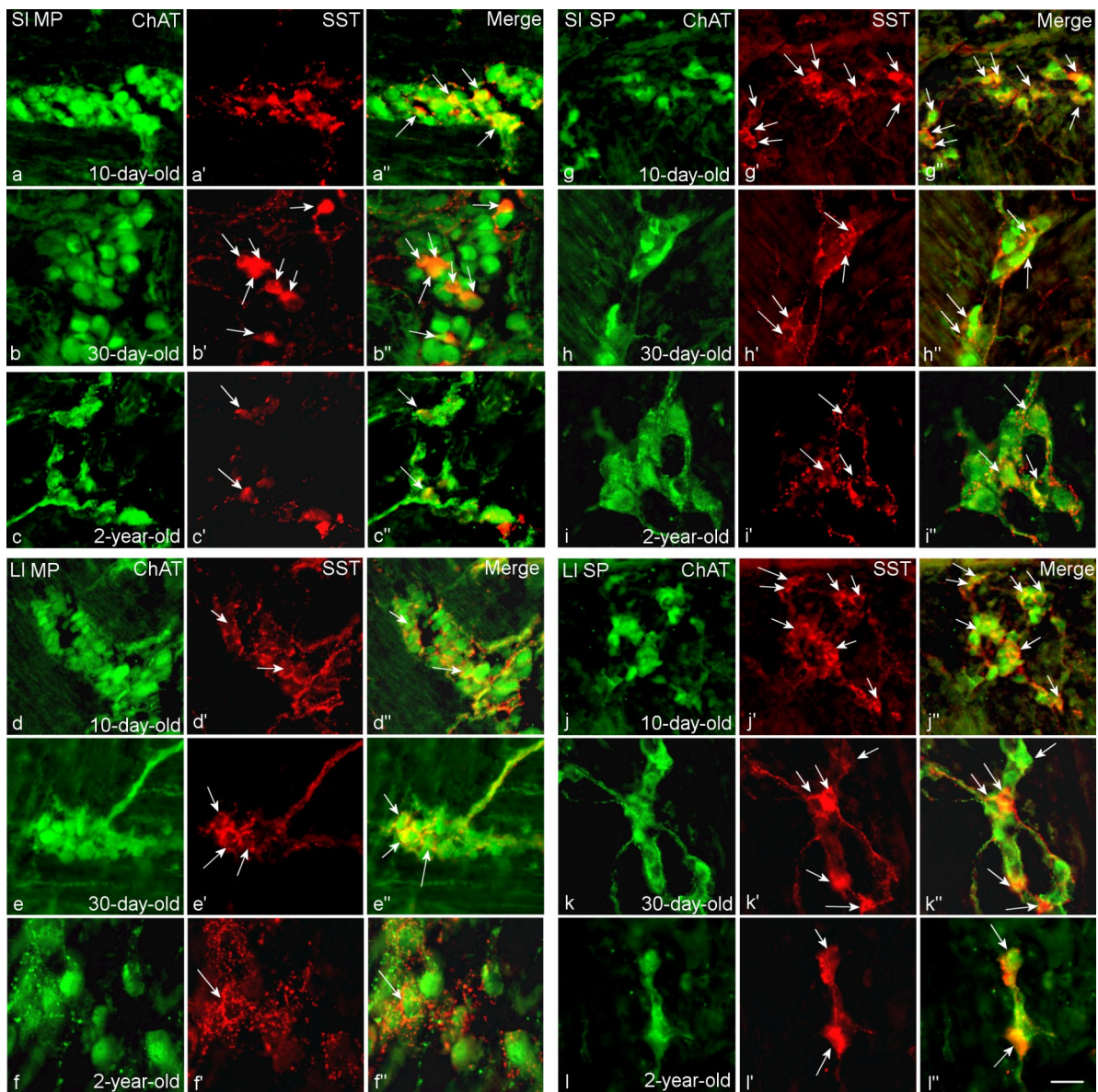


**Fig. 3** Fluorescence micrographs of SST (red) and ChAT (green) immunoreactivity in the MP (**a–f**) and SP (**g–l**) of SI (**a–c**, **g–i**) and LI (**d–f**, **j–l**) of 10-day-old (**a**, **g**, **d**, **j**), 30-day-old (**b**, **h**, **e**, **k**), and 2-year-old (**c**, **f**, **i**, **l**) rats. A letter without an apostrophe represents the

green channel, a letter with one apostrophe (') indicates the red channel, and a letter with two apostrophes (') denotes the merged image. SST-IR neurons are marked with arrows. Scale bar, 30  $\mu$ m

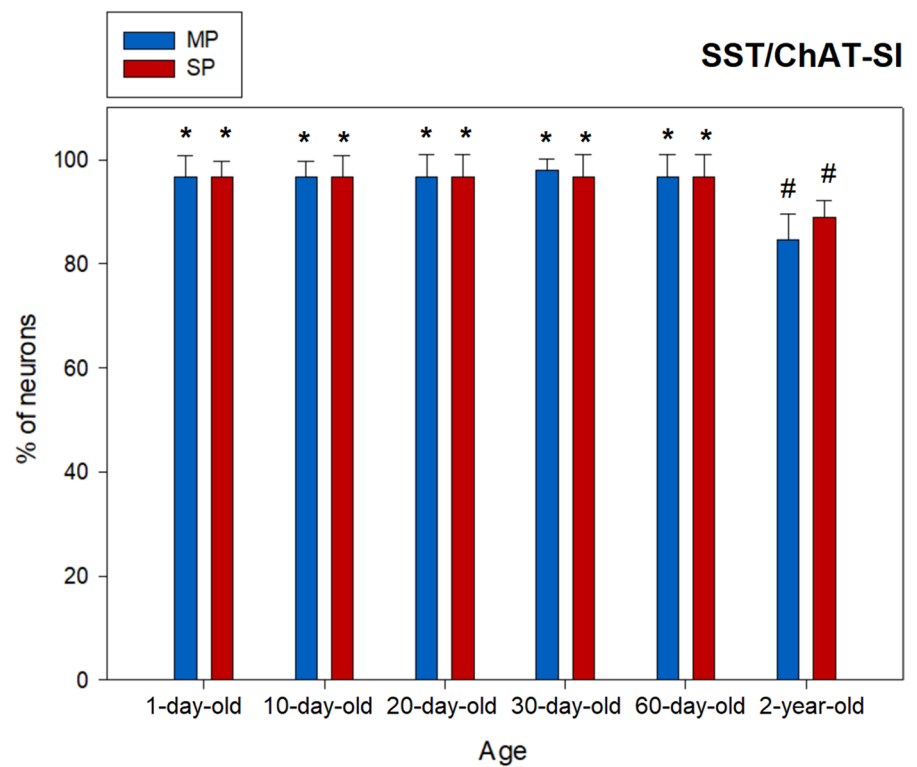
### SST/ChAT colocalization

The vast majority (97–98%) of SST-IR neurons were found to colocalize with ChAT from birth in both plexuses of the SI and LI (Figs. 3 and 4), where MC varied from  $0.97 \pm 0.01$  to  $0.98 \pm 0.02$ . We did not observe statistically significant differences among different age groups in the percentage of SST/ChAT-IR neurons in the MP and SP of both intestines from birth until 60 days of age. However, in aged rats, the percentage of SST-IR neurons colocalizing with ChAT decreased in both the MP [ $85 \pm 5.0$  (SI) and  $90 \pm 3.8$  (LI)]

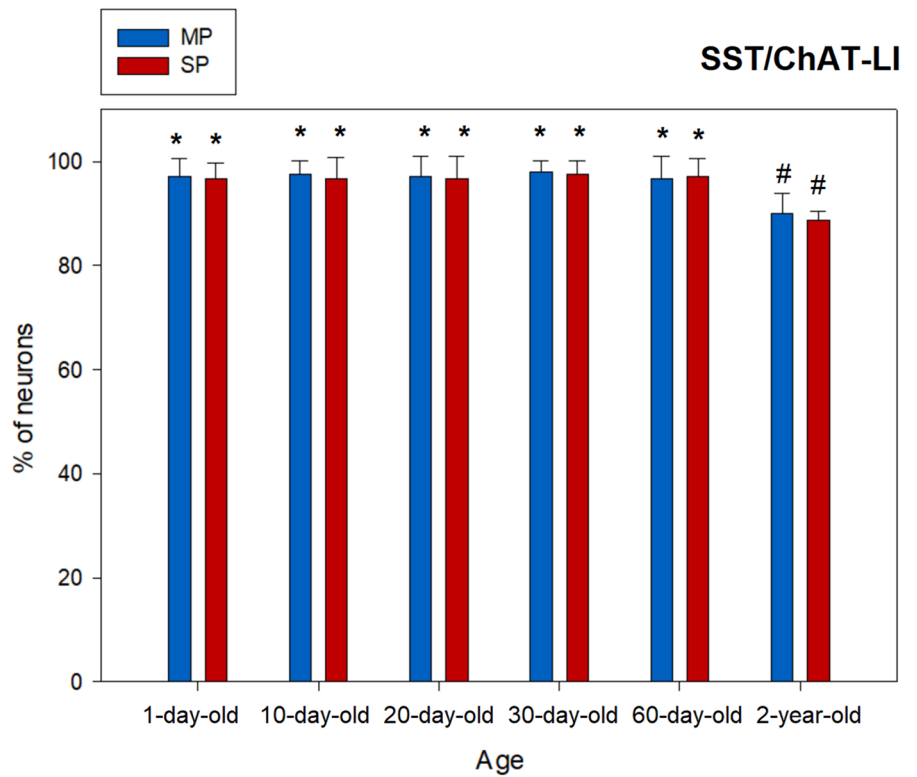
and SP [ $89 \pm 3.2$  (SI) and  $89 \pm 1.6$  (LI)] compared with younger animals [SI:  $p < 0.001$  (MP),  $p < 0.05$  (SP); LI:  $p < 0.05$  (MP),  $p < 0.05$  (SP)]. In aged rats, MC varied from  $0.82 \pm 0.07$  to  $0.91 \pm 0.03$ .

There were no statistically significant differences in the number of ChAT-IR neurons per ganglion in the MP of SI and LI during the first 60 days of life. However, in aged rats, the number of ChAT-IR neurons per ganglion significantly decreased from  $18.6 \pm 1.2$  to  $16.3 \pm 1.3$  in the SI and from  $19.5 \pm 1.4$  to  $17.1 \pm 1.4$  in the LI compared with 60-day-olds ( $p < 0.05$ ). In the SP of newborn

**Fig. 4** The percentage of SST-IR neurons colocalized ChAT in the SI (a) and LI (b) of rats at various ages.  $N=5$  in each age group (6 groups: 1-, 10-, 20-, 30-, 60-day-old and 2-year-old rats). One-way ANOVA, # $p < 0.05$  compared with newborn rats, \* $p < 0.05$  compared with 2-year-old rats



a



b



rats, a lower number of ChAT-IR neurons was observed ( $5.1 \pm 0.4$  SI and  $5.5 \pm 0.4$  LI) compared with 10-day-old rats ( $9.2 \pm 0.7$  SI and  $10.6 \pm 0.8$  LI) ( $p < 0.05$ ). We did not observe statistically significant differences in the number of SP ChAT-IR neurons between 10-day-old rats and older rats in either the SI or LI.

### SST/nNOS colocalization

In the MP, a small percentage of SST-IR neurons colocalized with nNOS from newborn ( $13 \pm 1.9$  (SI);  $3 \pm 2.0$  (LI);  $MC = 0.11 \pm 0.01$  SI,  $0.02 \pm 0.01$  LI) until 60 days of life ( $1 \pm 0.1$  (SI);  $2 \pm 1.8$  (LI);  $MC = 0.11 \pm 0.01$  SI,  $0.02 \pm 0.01$  LI) (Figs. 5 and 6). However, in aged rats, a large number of SST/nNOS-IR neurons were found ( $32 \pm 8.5$  (SI);  $23 \pm 6.7$

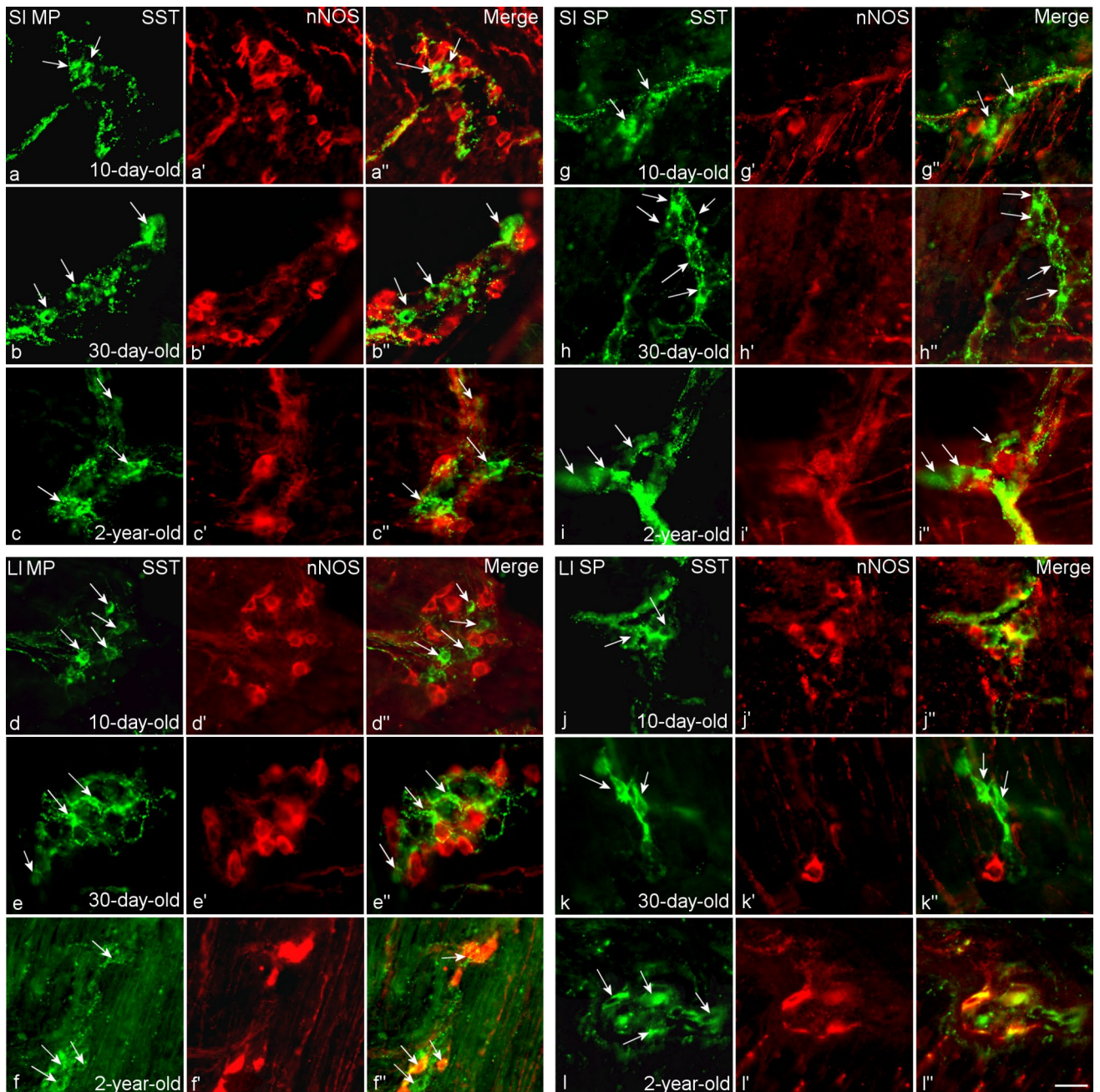
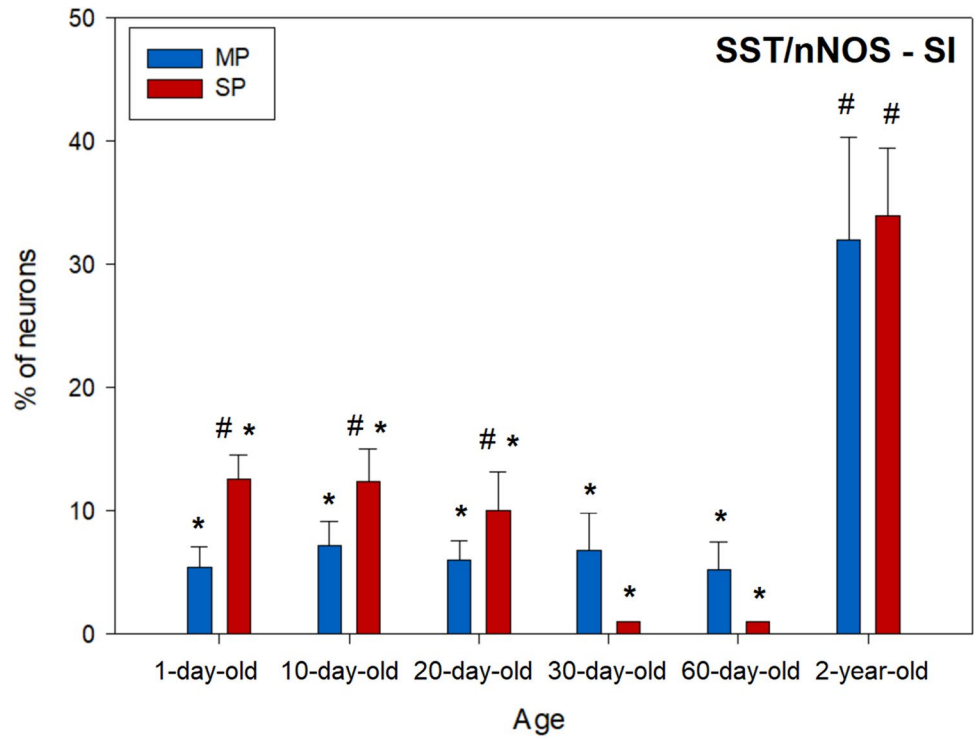


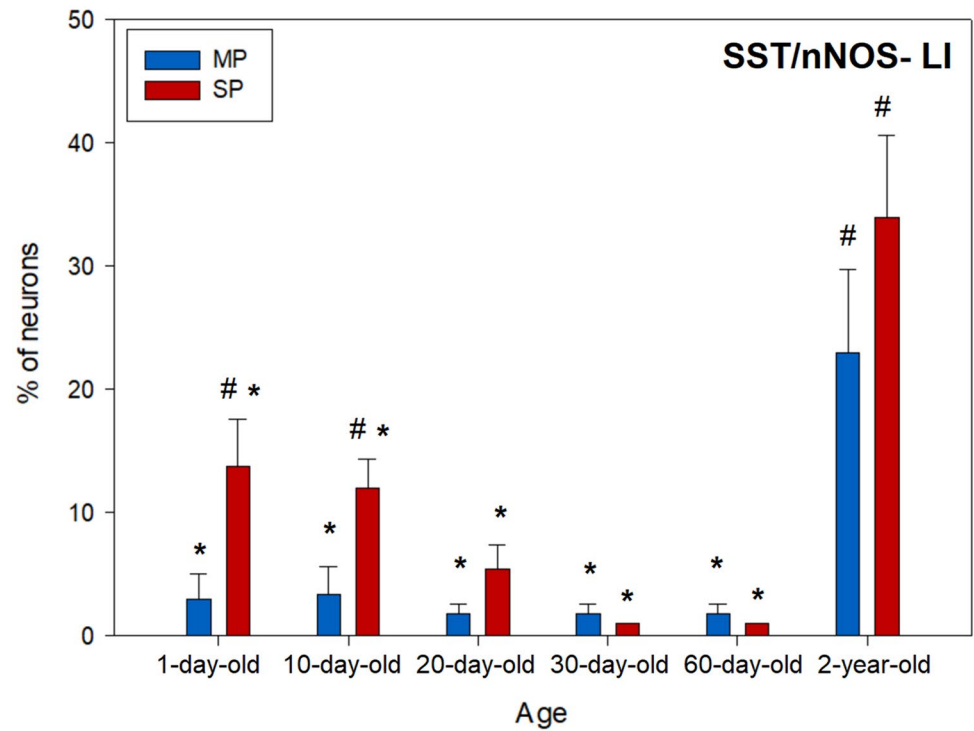
**Fig. 5** Fluorescence micrographs of SST (green) and nNOS (red) immunoreactivity in the MP (a–f) and SP (g–l) of SI (a–c, g–i) and LI (d–f, j–l) of 10-day-old (a, g, d, j), 30-day-old (b, h, e, k) and 2-year-old (c, f, i, l) rats. A letter without an apostrophe represents the

green channel; a letter with one apostrophe (') indicates the red channel; and a letter with two apostrophes (') denotes the merged image. SST-IR neurons are marked with arrows. Bar, 30  $\mu$ m

**Fig. 6** The percentage of SST-IR neurons colocalized nNOS in the SI (a) and LI (b) of rats at various ages.  $N=5$  in each age group (6 groups: 1-, 10-, 20-, 30-, 60-day-old and 2-year-old). One-way ANOVA, # $p < 0.05$  compared with newborn rats, \* $p < 0.05$  compared with 2-year-old rats



a



b

(LI); MC =  $0.36 \pm 0.03$  SI,  $0.31 \pm 0.04$  LI). The differences in the percentage of SST-IR neurons between aged animals and rats at 1, 10, 20, 30, and 60 days old were statistically significant ( $p < 0.001$  for both SI and LI in each age group).

In the SP, the proportion of SST/nNOS neurons notably decreased from 10-day-old rats ( $12 \pm 2.3$ ) to 30-day-old rats ( $1 \pm 0.1$ ) in the LI (MC decreased from  $0.14 \pm 0.01$  to  $0.01 \pm 0.01$ ) and from 20-day-old rats ( $10 \pm 3.2$ ) to 30-day-old rats ( $1 \pm 0.1$ ) in the SI (MC decreased from  $0.12 \pm 0.02$  to  $0.01 \pm 0.01$ ) (Figs. 5 and 6). Similar to the findings in the MP, in aged rats, the percentage of SST/nNOS neurons was high ( $34 \pm 5.5$  (SI);  $34 \pm 6.7$  (LI), MC =  $0.38 \pm 0.04$  SI,  $0.31 \pm 0.03$  LI) and significantly different from other age groups, including 1-, 10-, 20-, 30- and 60-day-old rats ( $p < 0.001$  for both SI and LI in each age group).

The largest number of nNOS-IR neurons per ganglion was found in newborn rats ( $8.3 \pm 0.5$  in SI and  $12.3 \pm 0.9$  in LI). Subsequently, this number decreased during ontogenesis up to 60 days of life ( $5.8 \pm 0.4$  SI,  $6.3 \pm 0.4$  LI) and remained stable thereafter. In 1- and 10-day-old rats, the number of MP nNOS-IR neurons was significantly higher in the LI compared with the SI ( $p < 0.05$ ).

In the SP of the SI and LI, the largest number of nNOS-IR neurons was also observed in newborn animals ( $5.2 \pm 0.6$  SI,  $5.3 \pm 0.6$  LI). However, during the following 20 days, the number rapidly declined, with only a few neurons found in 20-, 30-day-old, and 2-month-old rats, where most ganglia were devoid of nNOS-IR cells. In aged rats, there was a significant increase in the number of nNOS-IR cells ( $5.4 \pm 0.4$  SI,  $6.3 \pm 0.6$  LI) ( $p < 0.001$ ).

### SST/NPY colocalization

In contrast to ChAT and nNOS, many SST-IR neurons colocalized with NPY (Figs. 7 and 8). However, the percentage of SST/NPY-IR neurons varied significantly throughout postnatal development (MC ranged from  $0.36 \pm 0.04$  to  $0.78 \pm 0.05$ ), and no statistically significant differences were found in this parameter between different age groups in the MP and SP of both intestines.

### SST/GFAP colocalization

In both plexuses, GFAP immunoreactivity appeared as a network surrounding the ganglion cells (Fig. 9). No colocalization of SST with GFAP was observed in any of the studied animals.

### The intensity of the immunofluorescence and cross-sectional area of IR neurons

The intensity of immunofluorescence did not change in the MP of the SI and LI ( $p > 0.05$ ). The mean cross-sectional

area of SST-, PGP9.5-, nNOS-, ChAT-, and NPY-IR profiles gradually increased in the MP and SP of the SI and LI from birth to senescence (Fig. 5). No statistically significant differences were observed in this parameter between different markers, between MP and SP or between the SI and LI in the same age group (Table 3).

## Discussion

The results have shown that SST-IR neurons were present in the MP and SP of rats from birth until senescence. Our data on the distribution of SST-IR neurons and fibers in the rat SI and LI resemble the findings obtained on enteric neurons of guinea pigs, where more SST-IR neurons in adult animals were located in the SP compared with the MP in both the SI and LI (Costa et al. 1980). The percentage of SST-IR neurons in the MP varied from 10% to 20% in different age groups, which is similar to the data of Heinicke and Kiernan (1990), where 1–6 SST-IR neurons per ganglion were observed.

In the MP and SP of both the SI and LI, the percentage of SST-IR neurons increased during early postnatal development and reached its peak in the first month of life. The proportion of SST-IR cells then decreased in 2-year-old animals. In our previous works, we observed neurochemical changes in enteric neurons, including the expression of calcium-binding proteins, NPY, and nNOS during postnatal development (Masliukov et al. 2017b; Budnik et al. 2020; Budnik and Masliukov 2023). We found that the expression of calcium-binding proteins calbindin and calretinin, along with NPY, increases in early development (Masliukov et al. 2017a; Budnik et al. 2020). In the SP of the small intestine, the proportion of NPY-IR neurons decreases with aging (Budnik et al. 2020), similar to our results on SST neurons in the current study.

According to our results, the number of PGP9.5-IR (pan-neuronal marker) cells remains stable in the MP during postnatal development. In the SP, both the number of PGP9.5-IR and ChAT-IR neurons increases in the first 10 days of postnatal life. These findings are consistent with studies of the SP, revealing that SP neurons develop at a later stage compared with those in the MP (Kapur et al. 1992).

The majority of SST-IR neurons colocalized with ChAT. Vannucchi and Faussone-Pellegrini (1996) reported that ChAT-IR neurons were present in the MP of the gut in newborns but absent in the SP, where they appeared only in the second week of life. However, other data suggest that cholinergic neurons are born first at very early ages, from embryonic days 8–15 (Pham et al. 1991). We observed a decrease in the percentage of SST-IR neurons colocalizing with ChAT in the MP and SP of the SI and LI in aged rats. Literature data indicate that the age-associated decrease in

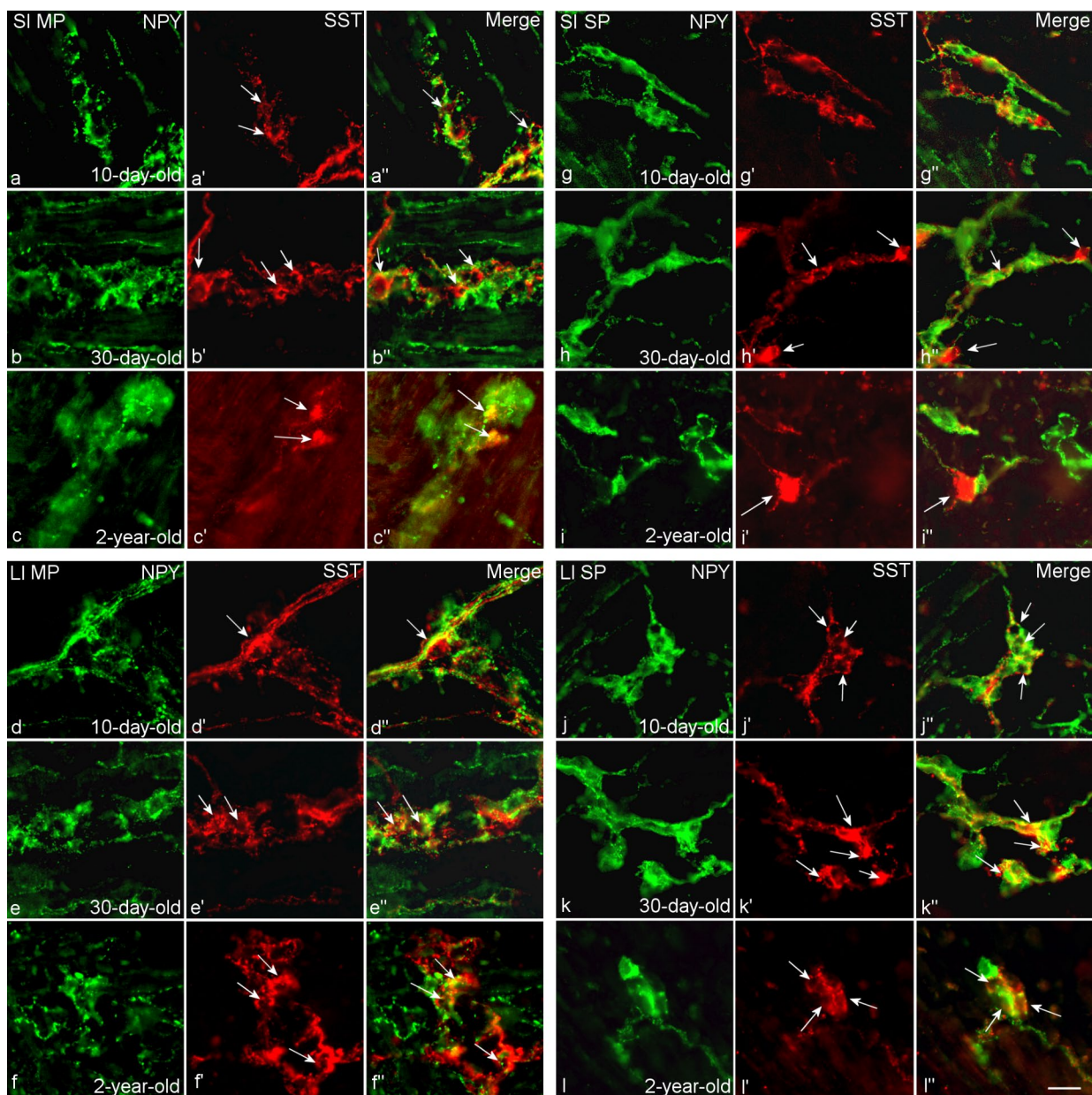


**Fig. 7** Fluorescence micrographs of SST (red) and NPY (green) immunoreactivity in the MP (a–f) and SP (g–l) of SI (a–c, g–i) and LI (d–f, j–l) of 10-day-old (a, g, d, j), 30-day-old (b, h, e, k), and 2-year-old (c, f, i, l) rats. A letter without an apostrophe represents the

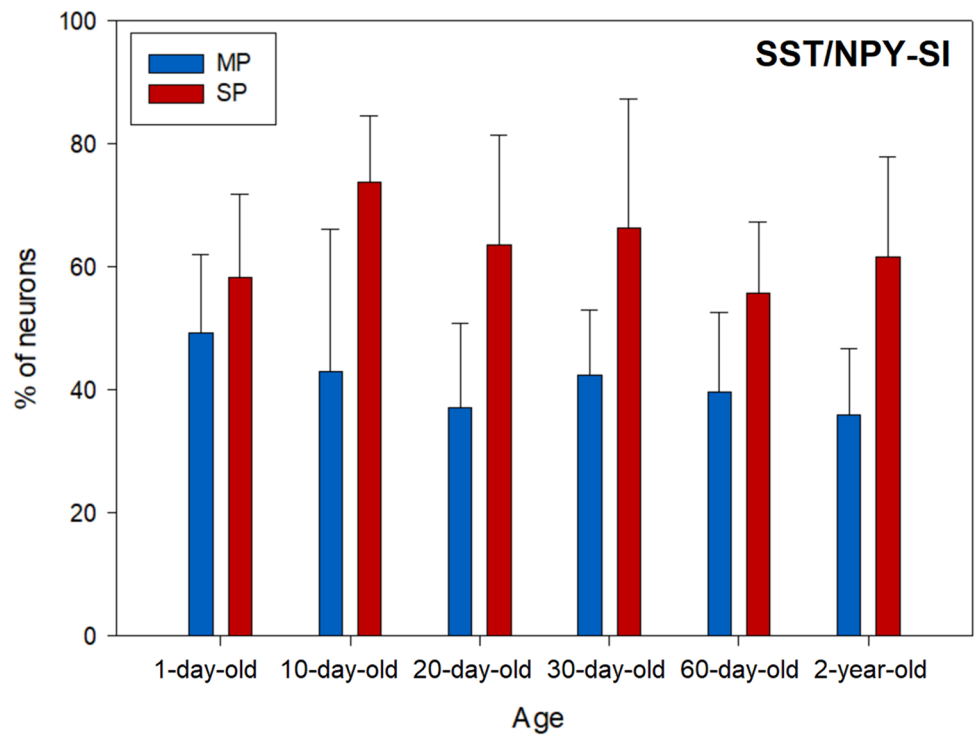
green channel, a letter with one apostrophe (') indicates the red channel, and a letter with two apostrophes (') denotes the merged image. SST-IR neurons are marked with arrows. Scale bar, 30  $\mu$ m

neuronal number in the MP is specific to ChAT-IR neurons in mice and humans (Nguyen et al. 2023).

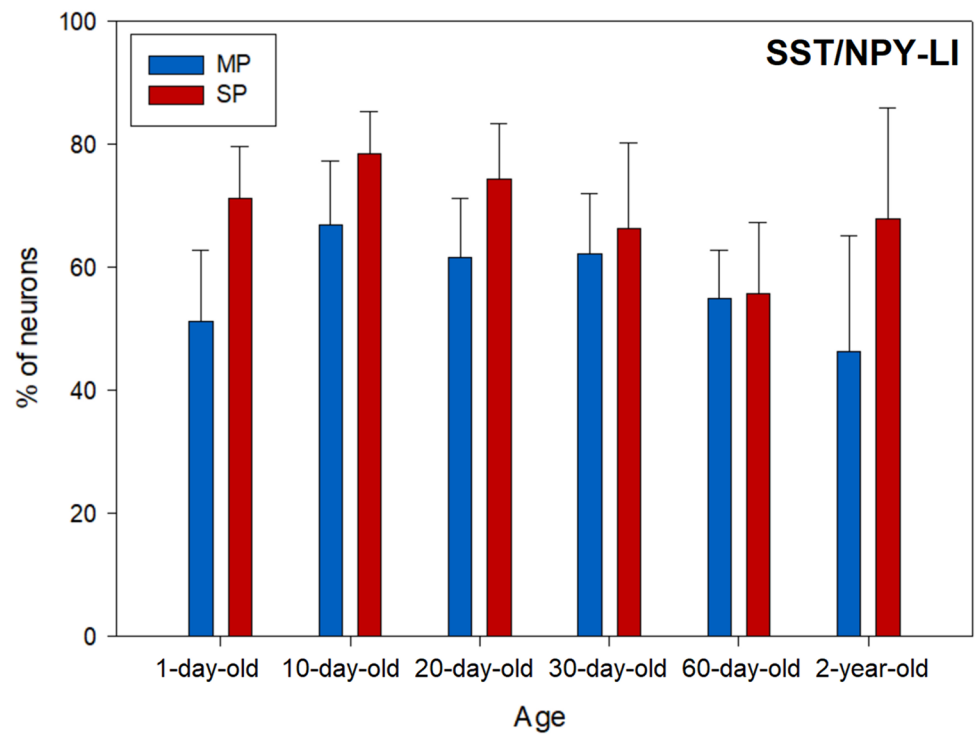
In humans, the number of SST-IR neurons varies in different types of enteric plexuses from 4% to 50% of the total neuronal population (Godlewski and Kaleczyc 2010; Kustermann et al. 2011). Treatment with somatostatin analogues could be effective in various pathological conditions of the gastrointestinal tract (Herszényi et al. 2013). SST analogues have shown effectiveness in treating patients with diarrhea associated with diabetes,

irritable bowel syndrome, and ileostomy (Camilleri 1996; McMahan et al. 2023). SST inhibits ion secretion, promotes water and sodium absorption in intestinal epithelial cells to improve diarrhea symptoms through inactivation of adenylate cyclase, inhibition of intracellular  $\text{Ca}^{2+}$  influx and  $\text{K}^{+}$  efflux via G-inhibiting protein, inhibition of active anion secretion, and stimulation of both  $\text{Na}^{+}$  and  $\text{Cl}^{-}$  absorption in the ileum (Xie et al. 2022). It also reduces the colonic tonic response in humans both in vivo and in vitro (Corleto 2010).

**Fig. 8** The percentage of SST-IR neurons colocalized NPY in the SI (a) and LI (b) of rats at various ages. *N*=5 in each age group (6 groups: 1-, 10-, 20-, 30-, 60-day-old and 2-year-old). One-way ANOVA, no statistically significant differences were found between age groups



a



b

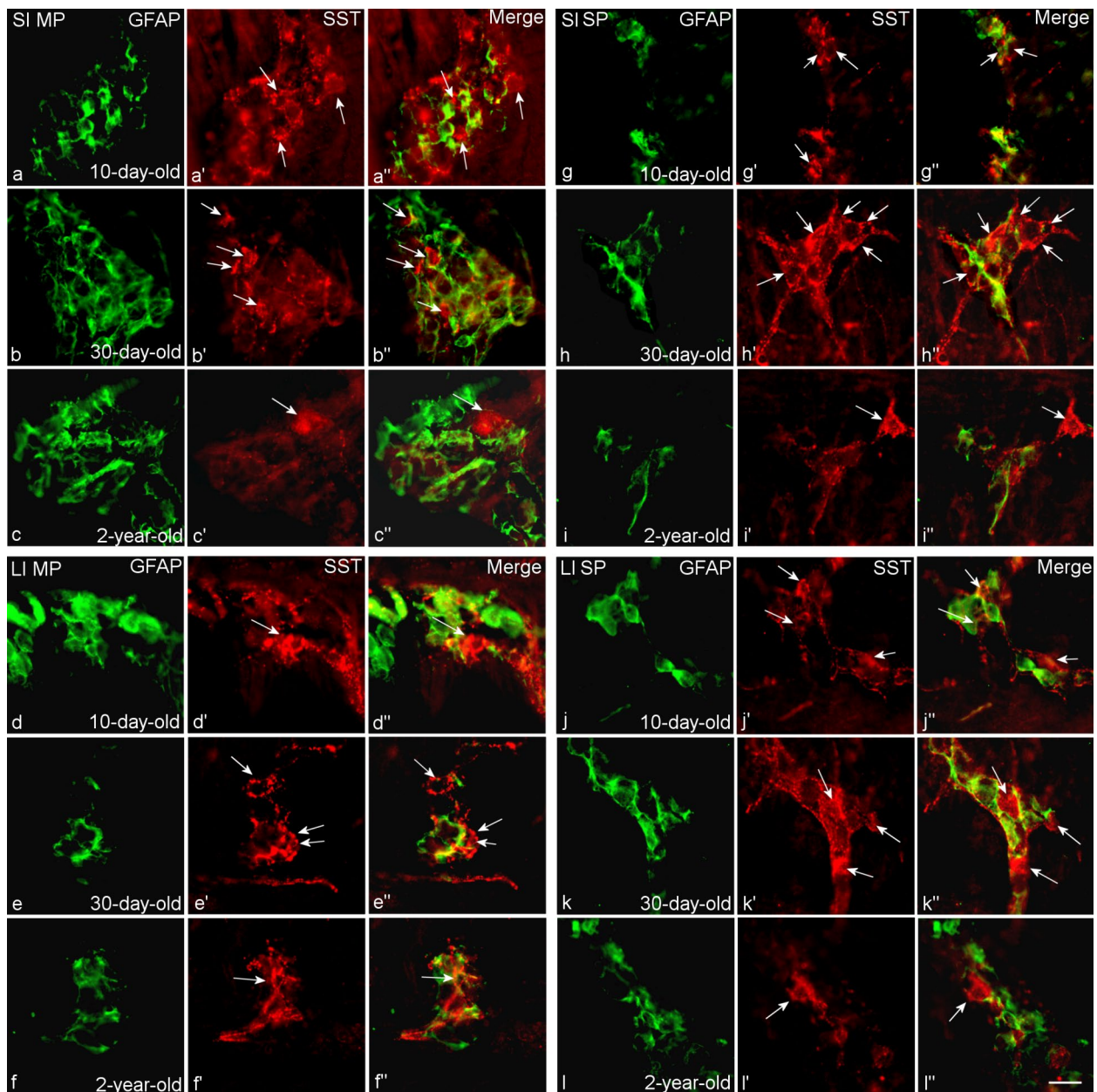


**Fig. 9** Fluorescence micrographs of SST (red) and GFAP (green) immunoreactivity in the MP (**a–f**) and SP (**g–l**) of SI (**a–c**, **g–i**) and LI (**d–f**, **j–l**) of 10-day-old (**a**, **g**, **d**, **j**), 30-day-old (**b**, **h**, **e**, **k**) and 2-year-old (**c**, **f**, **i**, **l**) rats. A letter without an apostrophe represents the

green channel, a letter with one apostrophe (') indicates the red channel, and a letter with two apostrophes (') denotes the merged image. SST-IR neurons are marked with arrows. Scale bar, 30  $\mu$ m

A small number of SST-IR neurons colocalize with nNOS in young rats from birth until 20 days of age. However, in aged rats, we observed a large number of SST/nNOS-IR neurons. These findings are consistent with our prior results indicating a higher number of nNOS-IR neurons in newborn rats compared with 30-day-old and 60-day-old animals and a significant increase in nNOS expression in aged neurons in the MP and SP of the SI and LI (Budnik and Masliukov 2023). Constipation, often observed in elderly individuals,

may be linked to increased production of NO by enteric neurons, which can suppress gut motility. Moreover, a high level of NO as a free radical supports inflammation (Dawson and Dawson 2018). In this scenario, a reduction in SST expression could be a compensatory mechanism to balance the overproduction of NO, as both have inhibitory effects on the gut.

Enteric glial cells contain GFAP, similar to astrocytes in the CNS (Björklund et al. 1984). In our study, we did

**Table 3** Cross-sectional areas of IR neurons in rats of different ages

Age	SST	PGP9.5	ChAT	nNOS	NPY
a) Cross-sectional areas of IR neurons in the MP of the SI ( $n = 100$ in each age group)					
Newborn rats	88 ± 4	94 ± 8	96 ± 6	84 ± 5	96 ± 6
10-day-old rats	92 ± 4	105 ± 6	108 ± 6	103 ± 9	101 ± 6
20-day-old rats	120 ± 6*	119 ± 9*	125 ± 9*	111 ± 7*	118 ± 9*
30-day-old rats	152 ± 7*	165 ± 11*	157 ± 11*	154 ± 9*	165 ± 10*
2-month-old rats	168 ± 14*	171 ± 18*	185 ± 18*	177 ± 10*	175 ± 12*
2-year-old rats	179 ± 15*	178 ± 15*	188 ± 15*	181 ± 12*	191 ± 13*
b) Cross-sectional areas of IR neurons in the SP of the SI ( $n = 100$ in each age group)					
Newborn rats	82 ± 5	80 ± 4	86 ± 5	79 ± 5	78 ± 7
10-day-old rats	79 ± 4	83 ± 6	81 ± 6	82 ± 9	81 ± 6
20-day-old rats	117 ± 7*	123 ± 8*	120 ± 8*	119 ± 10*	121 ± 8*
30-day-old rats	149 ± 7*	155 ± 12*	158 ± 11*	150 ± 9*	149 ± 8*
2-month-old rats	172 ± 14*	182 ± 18*	179 ± 12*	191 ± 13*	188 ± 11*
2-year-old rats	189 ± 15*	195 ± 15*	193 ± 15*	201 ± 12*	198 ± 12*
c) Cross-sectional areas of IR neurons in the MP of the LI ( $n = 100$ in each age group)					
Newborn rats	91 ± 5	89 ± 6	90 ± 4	88 ± 6	91 ± 7
10-day-old rats	89 ± 6	92 ± 5	94 ± 4	90 ± 4	88 ± 8
20-day-old rats	122 ± 8*	138 ± 9*	139 ± 9*	141 ± 10*	125 ± 8*
30-day-old rats	156 ± 8*	170 ± 12*	171 ± 10*	165 ± 8*	175 ± 11*
2-month-old rats	174 ± 10*	182 ± 18*	180 ± 18*	178 ± 10*	181 ± 9*
2-year-old rats	186 ± 15*	190 ± 15*	192 ± 12*	189 ± 12*	188 ± 12*
d) Cross-sectional areas of IR neurons in the SP of the LI ( $n = 100$ in each age group)					
Newborn	79 ± 5	82 ± 6	78 ± 6	86 ± 5	82 ± 4
10-day-old rats	82 ± 4	84 ± 6	84 ± 6	88 ± 9	84 ± 8
20-day-old rats	121 ± 6*	126 ± 9*	122 ± 8*	120 ± 8*	116 ± 11*
30-day-old rats	156 ± 7*	148 ± 10*	150 ± 9*	152 ± 11*	161 ± 9*
2-month-old rats	181 ± 14*	176 ± 12*	192 ± 12*	185 ± 13*	180 ± 12*
2-year-old rats	205 ± 10*	198 ± 11*	189 ± 15*	188 ± 11*	196 ± 12*

\* $P < 0.05$ , compared with newborn rats

not observe colocalization of SST with GFAP in rats of different ages from birth to senescence. Therefore, in the enteric nervous system, SST is present in neurons but not in glial cells. Nonetheless, approximately 90% of SST in the gastrointestinal tract is located in enteroendocrine cells rather than enteric neurons (Penman et al. 1983). However, SST-IR enteric neurons play a role in regulating intestinal motility, secretion, and inflammation (Van Op den Bosch et al., 2009; Gonkowski and Rytel 2019).

In the gut, SST reduces intestinal movement, water, and electrolyte secretion (Furness 2006; Gonkowski and Rytel 2019). Its inhibitory effect involves the suppression of cholinergic excitatory stimulation of secretomotor neurons coexisting with vasoactive intestinal peptide (VIP) (Foong et al. 2010). In rats, VIP is colocalized with NPY in the SP secretomotor neurons (Furness 2006). NPY, along with SST, inhibits gut motility and secretion (Furness 2006). No developmental changes were observed in the percentage of SST/NPY-IR neurons. It is worth noting

that many sympathetic neurons in the prevertebral ganglia innervating the gut also colocalize NPY and SST (Masliukov et al. 2023).

The aging of the gut is associated with microbiota dysbiosis and neuroinflammation (Nguyen et al. 2023). In pigs, SST expression increases during gut inflammation (Gonkowski and Całka 2010; Palus et al. 2017). SST is known to reduce inflammation by inhibiting T lymphocyte activity, granulocyte proliferation, the synthesis of proinflammatory cytokines, and the release of pain mediators, such as substance P and calcitonin gene-related peptide (Van Op den Bosch et al., 2009; Rai et al. 2015; Gonkowski and Rytel 2019). The decline in SST expression during aging may contribute to inflammatory processes in the gut of elderly individuals. Concentrations of SST immunoreactivity in the mucosa-submucosa of the descending colon were significantly reduced in ulcerative colitis and Crohn's colitis compared with a normal colon (Koch et al. 1988).

## Conclusions

SST expression in enteric neurons increases in young rats and decreases in senescence, accompanied by changes in colocalization with ChAT and nNOS. Colocalization of SST decreases with ChAT and increases with nNOS in aging. These changes may play a compensatory role and have pro-inflammatory effects in senescence.

**Acknowledgements** This work was supported by Russian Science Foundation, grant 23-25-00141, <https://rscf.ru/en/project/23-25-00141/>.

**Author contributions** A.I.E.—performing the experiments, data acquisition and analysis, and writing and editing; A.F.B.—performing the experiments, data acquisition, and analysis; P.M.M.—project design, supervision, funding acquisition, interpretation of results, writing the manuscript, and editing.

**Funding** Russian Science Foundation, grant 23-25-00141.

**Data availability** No datasets were generated or analyzed during the current study.

## Declarations

**Conflict of interest** The authors declare no competing interests.

**Ethical approval** The current study was approved by the Yaroslavl State Medical University. All procedures involving animals were conducted in accordance with the ethical standards of the institution.

## References

- Ampofo E, Nalbach L, Menger MD, Laschke MW (2020) Regulatory mechanisms of somatostatin expression. *Int J Mol Sci* 21:4170. <https://doi.org/10.3390/ijms21114170>
- Barrenschee M, Böttner M, Harde J, Lange C, Cossais F, Ebsen M, Vogel I, Wedel T (2015) SNAP-25 is abundantly expressed in enteric neuronal networks and upregulated by the neurotrophic factor GDNF. *Histochem Cell Biol* 143:611–623. <https://doi.org/10.1007/s00418-015-1310-x>
- Björklund H, Dahl D, Seiger A (1984) Neurofilament and glial fibrillary acid protein-related immunoreactivity in rodent enteric nervous system. *Neuroscience* 12:277–287. [https://doi.org/10.1016/0306-4522\(84\)90153-2](https://doi.org/10.1016/0306-4522(84)90153-2)
- Bolte S, Cordelières FP (2006) A guided tour into subcellular colocalization analysis in light microscopy. *J Microsc* 224:213–232. <https://doi.org/10.1111/j.1365-2818.2006.01706.x>
- Brazeau P, Vale W, Burgus R, Ling N, Butcher M, Rivier J, Guillemin R (1973) Hypothalamic polypeptide that inhibits the secretion of immunoreactive pituitary growth hormone. *Science* 179(4068):77–79. <https://doi.org/10.1126/science.179.4068.77>
- Budnik AF, Masliukov PM (2023) Postnatal development of the enteric neurons expressing neuronal nitric oxide synthase. *Anat Rec (hoboken)* 306:2276–2291. <https://doi.org/10.1002/ar.24947>
- Budnik AF, Aryaeva D, Vyshnyakova P, Masliukov PM (2020) Age related changes of neuropeptide Y-ergic system in the rat duodenum. *Neuropeptides* 80:101982. <https://doi.org/10.1016/j.npep.2019.101982>
- Camilleri M (1996) Effects of somatostatin analogues on human gastrointestinal motility. *Digestion* 57(Suppl 1):90–92. <https://doi.org/10.1159/000201407>
- Cao S, Li M, Sun Y, Wu P, Yang W, Dai H, Guo Y, Ye Y, Wang Z, Xie X, Chen X, Liang W (2022) Intermittent fasting enhances hippocampal NPY expression to promote neurogenesis after traumatic brain injury. *Nutrition* 97:111621. <https://doi.org/10.1016/j.nut.2022.111621>
- Corleto VD (2010) Somatostatin and the gastrointestinal tract. *Curr Opin Endocrinol Diabetes Obes* 17:63–68. <https://doi.org/10.1097/MED.0b013e32833463ed>
- Costa M, Furness JB, Smith II, Davies B, Oliver J (1980) An immunohistochemical study of the projections of somatostatin-containing neurons in the guinea-pig intestine. *Neuroscience* 5:841–852. [https://doi.org/10.1016/0306-4522\(80\)90153-0](https://doi.org/10.1016/0306-4522(80)90153-0)
- Dawson TM, Dawson VL (2018) Nitric oxide signaling in neurodegeneration and cell death. *Adv Pharmacol* 82:57–83. <https://doi.org/10.1016/bs.apha.2017.09.003>
- Dunn KW, Kamocka MM, McDonald JH (2011) A practical guide to evaluating colocalization in biological microscopy. *Am J Physiol Cell Physiol* 300:C723–C742. <https://doi.org/10.1152/ajpcell.00462.2010>
- Fatima M, Ren X, Pan H, Slade HFE, Asmar AJ, Xiong CM, Shi A, Xiong AE, Wang L, Duan B (2019) Spinal somatostatin-positive interneurons transmit chemical itch. *Pain* 160(5):1166–1174. <https://doi.org/10.1097/j.pain.0000000000001499>
- Fazi B, Biancolella M, Mehdawy B, Corazzari M, Minella D, Blandini F, Moreno S, Nardacci R, Nisticò R, Sepe S, Novelli G, Piacentini M, Di Sano F (2010) Characterization of gene expression induced by RTN-1C in human neuroblastoma cells and in mouse brain. *Neurobiol Dis* 40:634–644. <https://doi.org/10.1016/j.nbd.2010.08.007>
- Foo KS, Hellysaz A, Broberger C (2014) Expression and colocalization patterns of calbindin-D28k, calretinin and parvalbumin in the rat hypothalamic arcuate nucleus. *J Chem Neuroanat* 61–62:20–32. <https://doi.org/10.1016/j.jchemneu.2014.06.008>
- Foong JP (2016) Postnatal development of the mouse enteric nervous system. *Adv Exp Med Biol* 891:135–143. [https://doi.org/10.1007/978-3-319-27592-5\\_13](https://doi.org/10.1007/978-3-319-27592-5_13)
- Foong JP, Parry LJ, Bornstein JC (2010) Activation of neuronal SST<sub>1</sub> and SST<sub>2</sub> receptors decreases neurogenic secretion in the guinea-pig jejunum. *Neurogastroenterol Motil* 22(1209–1216):e317. <https://doi.org/10.1111/j.1365-2982.2010.01566.x>
- Furness JB (2006) *The enteric nervous system*. Blackwell Publishing, Oxford
- Furness JB, Stebbing MJ (2018) *The first brain: Species comparisons and evolutionary implications for the enteric and central nervous systems*. *Neurogastroenterol Motil*. <https://doi.org/10.1111/nmo.13234>
- Godlewski J, Kaleczyc J (2010) Somatostatin, substance P and calcitonin gene-related peptide-positive intramural nerve structures of the human large intestine affected by carcinoma. *Folia Histochem Cytobiol* 48:475–483. <https://doi.org/10.2478/v10042-010-0079-y>
- Gonkowski S, Całka J (2010) Changes in the somatostatin (SOM)-like immunoreactivity within nervous structures of the porcine descending colon under various pathological factors. *Exp Mol Pathol* 88:416–423. <https://doi.org/10.1016/j.yexmp.2010.01.011>
- Gonkowski S, Rytel L (2019) Somatostatin as an active substance in the mammalian enteric nervous system. *Int J Mol Sci* 20:4461. <https://doi.org/10.3390/ijms20184461>
- Guyer RA, Stavely R, Robertson K, Bhave S, Mueller JL, Picard NM, Hotta R, Kaltschmidt JA, Goldstein AM (2023) Single-cell multiome sequencing clarifies enteric glial diversity and identifies an intraganglionic population poised for neurogenesis. *Cell Rep* 42:112194. <https://doi.org/10.1016/j.celrep.2023.112194>



- Hao MM, Young HM (2009) Development of enteric neuron diversity. *J Cell Mol Med* 13:1193–1210. <https://doi.org/10.1111/j.1582-4934.2009.00813.x>
- Hao MM, Bornstein JC, Young HM (2013) Development of myenteric cholinergic neurons in ChAT-Cre;R26R-YFP mice. *J Comp Neurol* 521:3358–3370. <https://doi.org/10.1002/cne.23354>
- Heinicke EA, Kiernan JA (1990) An immunohistochemical study of the myenteric plexus of the colon in the rat and mouse. *J Anat* 170:51–62
- Herszényi L, Mihály E, Tulassay Z (2013) Somatostatin and the digestive system. Clinical experiences. *Orv Hetil* 154:1535–1540. <https://doi.org/10.1556/OH.2013.29721>
- Islam MN, Maeda N, Miyasato E, Jahan MR, Tarif AMM, Ishino T, Nozaki K, Masumoto KH, Yanai A, Shinoda K (2020) Expression of huntingtin-associated protein 1 in adult mouse dorsal root ganglia and its neurochemical characterization in reference to sensory neuron subpopulations. *IBRO Rep* 9:258–269. <https://doi.org/10.1016/j.ibror.2020.10.001>
- Kapur RP, Yost C, Palmiter RD (1992) A transgenic model for studying development of the enteric nervous system in normal and aganglionic mice. *Development* 116(1):167–175. <https://doi.org/10.1242/dev.116.Supplement.167>
- Kiss J, Csaba Z, Csáki A, Halász B (2006) Glutamatergic innervation of growth hormone-releasing hormone-containing neurons in the hypothalamic arcuate nucleus and somatostatin-containing neurons in the anterior periventricular nucleus of the rat. *Brain Res Bull* 70:278–288. <https://doi.org/10.1016/j.brainresbull.2006.05.006>
- Koch TR, Carney JA, Morris VA, Go VL (1988) Somatostatin in the idiopathic inflammatory bowel diseases. *Dis Colon Rectum* 31:198–203. <https://doi.org/10.1007/BF02552546>
- Kumar U (2023) Somatostatin and somatostatin receptors in tumour biology. *Int J Mol Sci* 25:436. <https://doi.org/10.3390/ijms25010436>
- Kustermann A, Neuhuber W, Brehmer A (2011) Calretinin and somatostatin immunoreactivities label different human submucosal neuron populations. *Anat Rec (hoboken)* 294:858–869. <https://doi.org/10.1002/ar.21365>
- Lepousez G, Csaba Z, Bernard V, Loudes C, Videau C, Lacombe J, Epelbaum J, Viollet C (2010) Somatostatin interneurons delineate the inner part of the external plexiform layer in the mouse main olfactory bulb. *J Comp Neurol* 518:1976–1994. <https://doi.org/10.1002/cne.22317>
- Machado FA, Souza RF, Figliuolo VR, Coutinho-Silva R, Castelucci P (2023) Effects of experimental ulcerative colitis on myenteric neurons in P2X7-knockout mice. *Histochem Cell Biol* 160:321–339. <https://doi.org/10.1007/s00418-023-02208-2>
- Masliukov PM, Emanuilov AI, Madalievva LV, Moiseev KY, Bulbin AV, Korzina MB, Porseva VV, Korobkin AA, Smirnova VP (2014) Development of nNOS-positive neurons in the rat sensory and sympathetic ganglia. *Neuroscience* 256:271–281. <https://doi.org/10.1016/j.neuroscience.2013.10.013>
- Masliukov PM, Budnik AF, Nozdrachev AD (2017a) Developmental changes of neurotransmitter properties in sympathetic neurons. *Adv Gerontol* 30(3):347–355
- Masliukov PM, Moiseev K, Budnik AF, Nozdrachev AD, Timmermans JP (2017b) Development of Calbindin- and Calretinin-immunopositive neurons in the enteric ganglia of rats. *Cell Mol Neurobiol* 37(7):1257–1267. <https://doi.org/10.1007/s10571-016-0457-x>
- Masliukov PM, Emanuilov AI, Budnik AF (2023) Sympathetic innervation of the development, maturity, and aging of the gastrointestinal tract. *Anat Rec (hoboken)* 306:2249–2263. <https://doi.org/10.1002/ar.25015>
- McMahan ZH, Kulkarni S, Chen J, Chen JZ, Xavier RJ, Pasricha PJ, Khanna D (2023) Systemic sclerosis gastrointestinal dysmotility: risk factors, pathophysiology, diagnosis and management. *Nat Rev Rheumatol* 19:166–181. <https://doi.org/10.1038/s41584-022-00900-6>
- Mongardi Fantaguzzi C, Thacker M, Chiocchetti R, Furness JB (2009) Identification of neuron types in the submucosal ganglia of the mouse ileum. *Cell Tissue Res* 336:179–189. <https://doi.org/10.1007/s00441-009-0773-2>
- Nguyen TT, Baumann P, Tüscher O, Schick S, Endres K (2023) The aging enteric nervous system. *Int J Mol Sci* 24:9471. <https://doi.org/10.3390/ijms24119471>
- Palus K, Bulc M, Čalka J (2017) Changes in somatostatin-like immunoreactivity in the sympathetic neurons projecting to the prepyloric area of the porcine stomach induced by selected pathological conditions. *Biomed Res Int*. <https://doi.org/10.1155/2017/9037476>
- Pataký DM, Curtis SB, Buchan AM (1990) The co-localization of neuropeptides in the submucosa of the small intestine of normal Wistar and non-diabetic BB rats. *Neuroscience* 36:247–254. [https://doi.org/10.1016/0306-4522\(90\)90366-c](https://doi.org/10.1016/0306-4522(90)90366-c)
- Peng S, Wu WQ, Li LY, Shi YC, Lin S, Song ZY (2023) Deficiency of neuropeptide Y attenuates neointima formation after vascular injury in mice. *BMC Cardiovasc Disord* 23(1):239. <https://doi.org/10.1186/s12872-023-03267-y>
- Penman E, Wass JA, Butler MG, Penny ES, Price J, Wu P, Rees LH (1983) Distribution and characterisation of immunoreactive somatostatin in human gastrointestinal tract. *Regul Pept* 7:53–65. [https://doi.org/10.1016/0167-0115\(83\)90281-1](https://doi.org/10.1016/0167-0115(83)90281-1)
- Pham TD, Gershon MD, Rothman TP (1991) Time of origin of neurons in the murine enteric nervous system: sequence in relation to phenotype. *J Comp Neurol* 314:789–798. <https://doi.org/10.1002/cne.903140411>
- Rai U, Thrimawithana TR, Valery C, Young SA (2015) Therapeutic uses of somatostatin and its analogues: current view and potential applications. *Pharmacol Ther* 152:98–110. <https://doi.org/10.1016/j.pharmthera.2015.05.007>
- Real MA, Heredia R, Labrador Mdel C, Dávila JC, Guirado S (2009) Expression of somatostatin and neuropeptide Y in the embryonic, postnatal, and adult mouse amygdalar complex. *J Comp Neurol* 513:335–348. <https://doi.org/10.1002/cne.21970>
- Rosas-Arellano A, Villalobos-González JB, Palma-Tirado L, Beltrán FA, Cárabez-Trejo A, Missirlis F, Castro MA (2016) A simple solution for antibody signal enhancement in immunofluorescence and triple immunogold assays. *Histochem Cell Biol* 146:421–430. <https://doi.org/10.1007/s00418-016-1447-2>
- Scott-Solomon E, Boehm E, Kuruvilla R (2021) The sympathetic nervous system in development and disease. *Nat Rev Neurosci* 22:685–702. <https://doi.org/10.1038/s41583-021-00523-y>
- Van Op den Bosch J, Adriaensen D, Van Nassauw L, Timmermans JP (2009) The role(s) of somatostatin, structurally related peptides and somatostatin receptors in the gastrointestinal tract: a review. *Regul Pept* 156:1–8. <https://doi.org/10.1016/j.regpep.2009.04.003>
- Vannucchi MG, Faussone-Pellegrini MS (1996) Differentiation of cholinergic cells in the rat gut during pre- and postnatal life. *Neurosci Lett* 206:105–108. [https://doi.org/10.1016/s0304-3940\(96\)12440-x](https://doi.org/10.1016/s0304-3940(96)12440-x)
- Vishnyakova PA, Moiseev KY, Porseva VV, Pankrasheva LG, Budnik AF, Nozdrachev AD, Masliukov PM (2021) Somatostatin-expressing neurons in the tuberal region of rat hypothalamus during aging. *J Evol Biochem Phys* 57:1480–1489. <https://doi.org/10.1134/S0022093021060247>
- Warren TG, Shields D (1984) Expression of preprosomatostatin in heterologous cells: biosynthesis, posttranslational processing, and secretion of mature somatostatin. *Cell* 39:547–555. [https://doi.org/10.1016/0092-8674\(84\)90461-6](https://doi.org/10.1016/0092-8674(84)90461-6)

- Xie X, Geng C, Li X, Liao J, Li Y, Guo Y, Wang C (2022) Roles of gastrointestinal polypeptides in intestinal barrier regulation. *Peptides* 151:170753. <https://doi.org/10.1016/j.peptides.2022.170753>
- Xu Y, Liu J, He M, Liu R, Belegu V, Dai P, Liu W, Wang W, Xia QJ, Shang FF, Luo CZ, Zhou X, Liu S, McDonald J, Liu J, Zuo YX, Liu F, Wang TH (2016) Mechanisms of PDGF siRNA-mediated inhibition of bone cancer pain in the spinal cord. *Sci Rep* 6:27512. <https://doi.org/10.1038/srep27512>
- Yu J, Min D, Bai Y, Qu L, Zou T, Wang S (2020) Electroacupuncture alleviates Parkinson disease and regulates the expression of brain-gut peptides. *Exp Anim* 69:448–460. <https://doi.org/10.1538/expanim.19-0153>
- Zhang D, Chen Y, Wei Y, Chen H, Wu Y, Wu L, Li J, Ren Q, Miao C, Zhu T, Liu J, Ke B, Zhou C (2024) Spatial transcriptomics and single-nucleus RNA sequencing reveal a transcriptomic atlas of adult human spinal cord. *Elife* 12:RP92046. <https://doi.org/10.7554/eLife.92046>

**Publisher's Note** Springer Nature remains neutral with regard to jurisdictional claims in published maps and institutional affiliations.

Springer Nature or its licensor (e.g. a society or other partner) holds exclusive rights to this article under a publishing agreement with the author(s) or other rightsholder(s); author self-archiving of the accepted manuscript version of this article is solely governed by the terms of such publishing agreement and applicable law.